# The Design of Spherical 4R Linkages for Four Specified Orientations

D. Alan Ruth
and
J. Michael McCarthy

Robotics and Automation Laboratory
Department of Mechanical Engineering
University of California, Irvine
Irvine, California 92697-3975
jmmccart@uci.edu

**Summary.** This chapter describes a computer-aided design software system for spherical four-bar linkages that is based on Burmester's planar theory. The designer identifies a task in the form of four goal orientations for the floating link and the software generates an array of available linkages known as the Type Map. The equation of a spherical triangle provides a direct connection to the graphical techniques of Burmester. This paper further develops the linkage type characterization required for an assessment of the resulting designs.

**Keywords**. Burmester theory, spherical four-bar linkage, computer-aided design, rigid-body guidance, four specified orientations.

## 1. Introduction

In this chapter we describe the theoretical foundation of the design software `SphinxPC` which provides a convenient means to design spherical four-bar linkages to guide a body through four specified orientations (Fig. 1). These linkages can be viewed as spherical quadrilaterals with vertices that are hinged joints, denoted $R$ for *revolute*. The axes of these hinges must intersect in a single point in order for the spherical $4R$ linkage to provide a one degree-of-freedom rotational, or *spherical*, movement.

The design theory underlying our formulation parallels the complex number formulation of Sandor and Erdman (1984), which is the basis of the design software LINCAGES. Murray and McCarthy (1994) showed that the equation of a spherical triangle yields equivalent results for spherical linkage design, while McCarthy (1995) showed that their "standard form" equation is easily transformed into the equation of a planar triangle. This formulation has been implemented in the design software `SphinxPC` presented here.

### 1.1 Burmester Theory

A four-bar linkage is formed when the floating link of a two-jointed open chain, called an $RR$ dyad, is rigidly connected to the floating link of another

one, to form a closed $4R$ chain. Burmester (1886) formulated this problem as locating the center-points for $RR$ dyads that are compatible with a specified set of positions of the floating link. All the linkages that can be assembled by connecting the various dyads are solutions to the design problem. This approach is necessarily a two step process: First, the set of $RR$ chains is identified, and then, the associated $4R$ linkages are assembled and evaluated. This is called the "design of a guiding linkage" by Hall (1961), "rigid-body guidance" by Suh and Radcliffe (1978), and "motion generation" by Sandor and Erdman (1984).

In the late 70's and early 80's, researchers transformed Burmester's geometric design procedures into computer algorithms with interactive graphics. The first was Kaufman's KINSYN (Kaufman 1978), followed shortly by Erdman's LINCAGES package (Erdman and Gustafson 1977), and later by Waldron's RECSYN (Waldron and Song 1981). These programs rapidly compute the planar $RR$ dyads that reach a specified set of positions. Then, various strategies are used to evaluate and present the associated planar $4R$ linkages. The goal is to enable the inventor to quickly survey the dimensions and evaluate the movement of many different planar linkages that achieve the specified task (Erdman 1993). Our approach to spherical linkage design follows this same format.

### 1.2 The Design Methodology

The task for the spherical linkage is defined by four orientations. The computation of associated spherical $RR$ dyads is based on Roth's version of Burmester's theorem which states, in effect: The central-axis of a spherical $RR$ dyad "views" opposite sides of the complementary-axis quadrilateral in equal, or supplementary, angles (Bottema and Roth 1979). McCarthy (1995) shows that this theorem yields a construction that uses the *complementary-axis quadrilateral* as a "compatibility linkage" to generate central-axes. The result is a cubic cone of central-axes, called the *central-axis cone*.

Pairs of points on the central-axis cone define $4R$ linkages that reach the four specified orientations. The result is a two dimensional set of linkages that is displayed as a *Type Map*. Important characteristics of the overall movement of the linkage such as its type, and whether or not it passes through each position smoothly and in order are displayed by color coding. The designer interacts with the Type Map to select and examine various designs.

Our spherical linkage design process consists of three major phases: *i)* Task specification; *ii)* Type map generation; and *iii)* Design selection. See Figure 2.

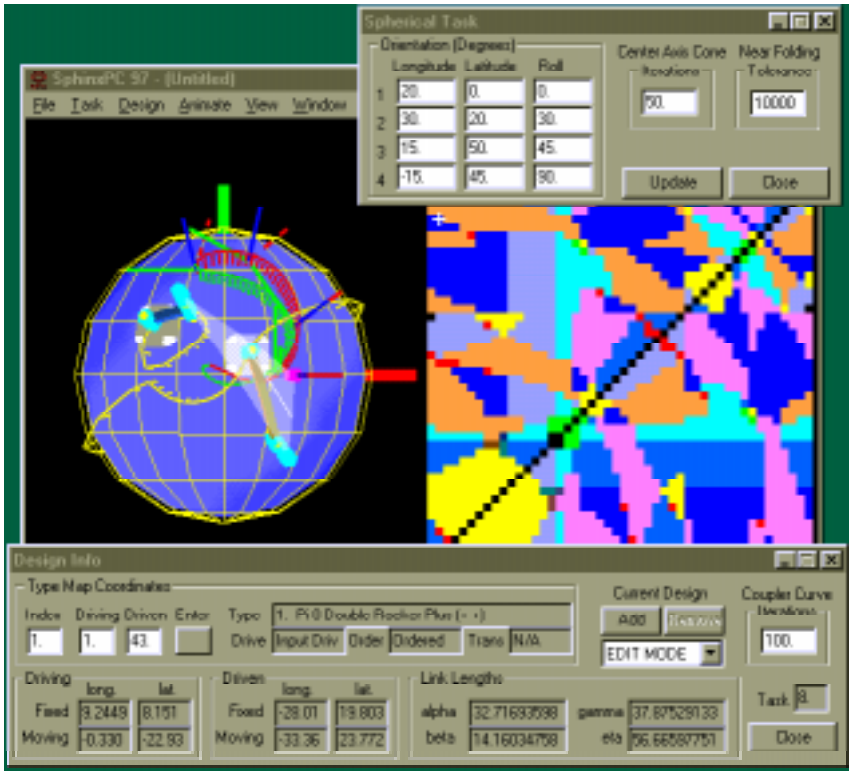


**Fig. 1.** The desk top of `SphinxPC` showing the workspace, type map, and the task and design dialog boxes.

## 2. Task Specification

The task for a spherical $4R$ linkage is defined in terms of a set of four orientations that the coupler link of the mechanism is to attain during its movement. Usually this consists of a start and a goal together with two intermediate orientations to guide the overall movement of the linkage. The task directly specifies, via the central-axis cone, all the spherical $RR$ dyads that can be used to assemble linkages.

Figure 3 shows the dialog box which allows input of the desired orientations. We use "longitude" and "latitude" angles to position the $Z$-axis of the moving frame and a rotation angle about this axis, called "roll," to define each orientation. These coordinates allow the use of a globe as a convenient visualization tool.

The primary steps in this phase of the design process are: *i)* Construct the compatibility linkage, and *ii)* Generate the central-axis cone.

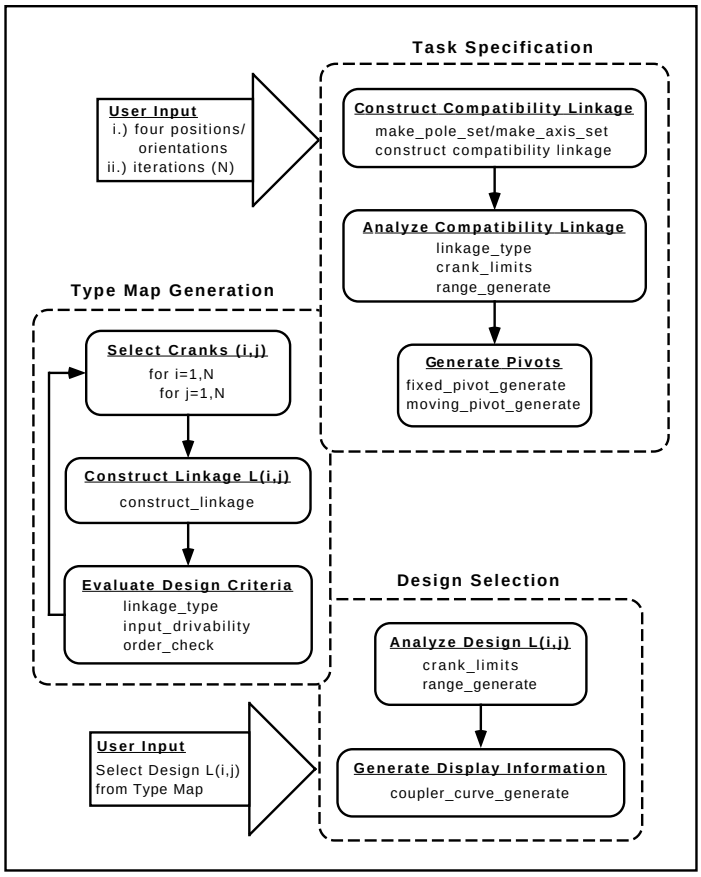


**Fig. 2.** Overview of spherical linkage design process implemented in `SphinxPC`.

### 2.1 Construct the Compatibility Linkage.

Given four orientations of the moving reference frame, we construct the relative rotations $[R_{12}]$, $[R_{23}]$, $[R_{34}]$ and $[R_{14}]$, and determine their rotation axes, $\mathbf{S}_{12}$, $\mathbf{S}_{23}$, $\mathbf{S}_{34}$, and $\mathbf{S}_{14}$. These axes define a spherical quadrilateral $\mathbf{S}_{12}\mathbf{S}_{23}\mathbf{S}_{34}\mathbf{S}_{14}$ known as a complementary-axis quadrilateral. We now consider this quadrilateral to be a spherical four-bar linkage (Figure 4), and use its configurations to determine the fixed axes compatible with the four orientations (McCarthy 1995). The angular lengths of the sides of this compatibility linkage are given by:

$$\begin{aligned} \alpha &= \arccos(\mathbf{S}_{12} \cdot \mathbf{S}_{23}), \quad \beta = \arccos(\mathbf{S}_{14} \cdot \mathbf{S}_{34}), \\ \gamma &= \arccos(\mathbf{S}_{12} \cdot \mathbf{S}_{14}), \quad \eta = \arccos(\mathbf{S}_{23} \cdot \mathbf{S}_{34}). \end{aligned} \tag{1}$$

Its initial configuration is defined by the crank angle $\theta$ and coupler angle $\phi$ given by:

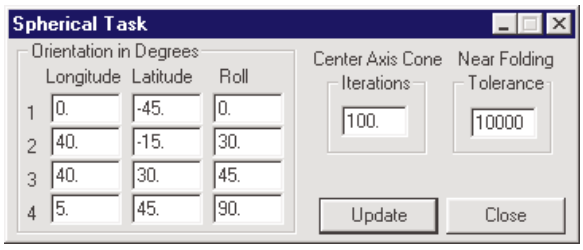


**Fig. 3.** The task of the linkage is defined by four orientations input through the Spherical Task dialog box.

$$\begin{aligned}\theta_0 &= \arctan \frac{(\mathbf{S}_{12} \times \mathbf{S}_{14}) \cdot \mathbf{S}_{23}}{(\mathbf{S}_{12} \times \mathbf{S}_{14}) \cdot (\mathbf{S}_{12} \times \mathbf{S}_{23})}, \\ \phi_0 &= \arctan \frac{(\mathbf{S}_{12} \times \mathbf{S}_{23}) \cdot \mathbf{S}_{34}}{(\mathbf{S}_{12} \times \mathbf{S}_{23}) \cdot (\mathbf{S}_{23} \times \mathbf{S}_{34})}. \end{aligned} \tag{2}$$

As the driving crank $\mathbf{S}_{12}\mathbf{S}_{23}$ rotates by the angle $\theta$, the coupler $\mathbf{S}_{23}\mathbf{S}_{34}$ takes various orientations allowed by the dimensions of the linkage. The relative rotation axis of the coupler from its initial orientation to every other orientation is a central-axis compatible with the four specified orientations.

### 2.2 Generate the Central-axis Cone

In order for a central-axis $\mathbf{G}$ to view the sides $\mathbf{S}_{12}\mathbf{S}_{23}$ and $\mathbf{S}_{14}\mathbf{S}_{34}$ in the same angle $\kappa$, it must satisfy a pair of equations, each defining a spherical triangle. Consider the spherical triangle with vertex $\mathbf{G}$ and the arc joining $\mathbf{S}_{12}\mathbf{S}_{23}$ as its base. Let the interior angles at each end of the base be $\Delta\theta/2$ and $\Delta\phi/2$. Similarly, consider the spherical triangle formed by $\mathbf{G}$ and the arc $\mathbf{S}_{14}\mathbf{S}_{34}$, with interior angles $\Delta\psi/2$ and $\Delta\zeta/2$. Then, to be a central-axis the coordinates of $\mathbf{G}$ must satisfy the equations:

$$\begin{aligned}\sin\kappa\mathbf{G} &= \sin\frac{\Delta\theta}{2}\cos\frac{\Delta\phi}{2}\mathbf{S}_{12} + \sin\frac{\Delta\phi}{2}\cos\frac{\Delta\theta}{2}\mathbf{S}_{23} \\ &\quad + \sin\frac{\Delta\theta}{2}\sin\frac{\Delta\phi}{2}\mathbf{S}_{12} \times \mathbf{S}_{23}, \\ \sin\kappa\mathbf{G} &= \sin\frac{\Delta\psi}{2}\cos\frac{\Delta\zeta}{2}\mathbf{S}_{14} + \sin\frac{\Delta\zeta}{2}\cos\frac{\Delta\psi}{2}\mathbf{S}_{34} \\ &\quad + \sin\frac{\Delta\psi}{2}\sin\frac{\Delta\zeta}{2}\mathbf{S}_{14} \times \mathbf{S}_{34}. \end{aligned} \tag{3}$$

These equations have a solution $\mathbf{G}$ when the angles $\theta$, $\phi$, $\zeta$ and $\psi$ are the configuration angles of the compatibility linkage (McCarthy 1995).

The constraint equation of the complementary-axis quadrilateral considered as a spherical four-bar linkage determines the coupler angle $\phi$ as a function of $\theta$, given by:

$$\phi(\theta) = \arctan(\frac{B}{A}) \pm \arccos(\frac{C}{\sqrt{A^2 + B^2}}) \tag{4}$$

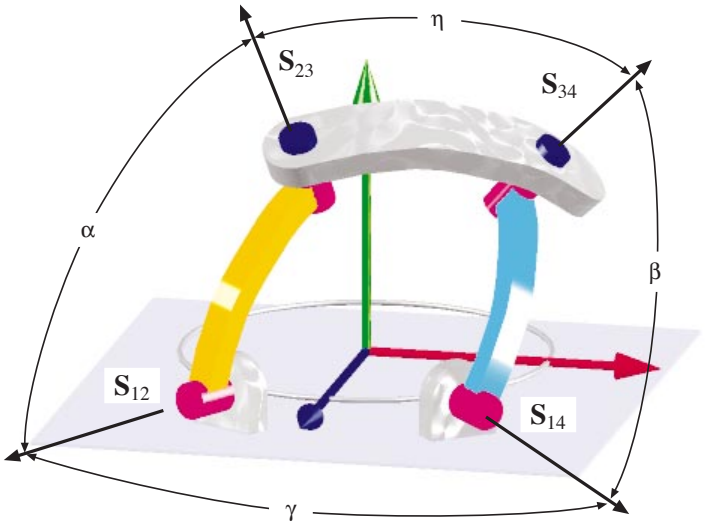


**Fig. 4.** The complementary-axis quadrilateral is used as a spherical 4R linkage to compute the central-axis cone.

where

$$\begin{aligned} A(\theta) &= \sin\eta(\sin\gamma\cos\alpha\cos\theta - \sin\alpha\cos\gamma), \\ B(\theta) &= -\sin\eta\sin\gamma\sin\theta, \\ C(\theta) &= \cos\beta - \cos\eta(\sin\alpha\sin\gamma\cos\theta + \cos\alpha\cos\gamma). \end{aligned} \tag{5}$$

The result is a parameterized equation of the central-axis cone:

$$\begin{aligned} \sin\frac{\beta}{2}\mathbf{G} &= \sin\frac{\Delta\theta}{2}\cos\frac{\Delta\phi(\theta)}{2}\mathbf{S}_{12} + \sin\frac{\Delta\phi(\theta)}{2}\cos\frac{\Delta\theta}{2}\mathbf{S}_{23} \\ &\quad + \sin\frac{\Delta\theta}{2}\sin\frac{\Delta\phi(\theta)}{2}\mathbf{S}_{12}\times\mathbf{S}_{23}, \end{aligned} \tag{6}$$

where $\Delta\theta = \theta - \theta_O$ and $\Delta\phi = \phi - \phi_0$.

**2.2.1 Set the Bias for Each Axis.** The fixed axes defined in Eq. (6) can be distinguished by whether or not they are directed toward the $Z > 0$ hemisphere. This provides a convenient way to keep track of the 16 equivalent forms that exist for a given spherical quadrilateral. By biasing all the axes toward the $Z > 0$ hemisphere, we can defined each of the various forms of the linkage by negating combinations of the four axes. Associated with each form is a different Type Map that can be selected by the designer.

To ensure that the central-axes are biased toward $Z > 0$, we identify the intersection of the central-axis cone with the $Z = 0$ plane, as the starting point for the cone generation routine. This intersection is obtained by solving the algebraic equation of the central-axis cone which becomes a cubic polynomial in the $X$-component of the central-axis:

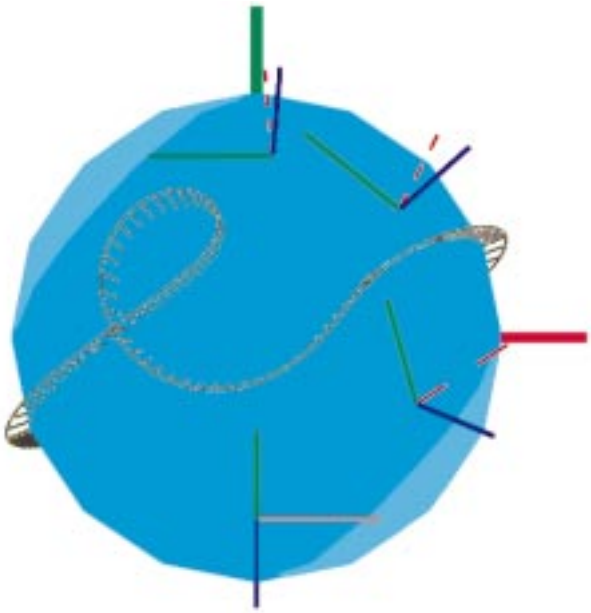

**Fig. 5.** The central-axis cone is the set of fixed axes of spherical $RR$ dyads compatible with four specified orientations.

$$C_1 x^3 + C_2 x^2 + C_3 x + C_4 = 0, \tag{7}$$

where

$$\begin{aligned}
C_1 &= -r_1q_2q_3q_4 + r_2q_1q_3q_4 + r_3q_1q_2q_4 - r_4q_1q_2q_3 + \\
&\quad q_1r_2r_3r_4 - q_2r_1r_3r_4 - q_3r_1r_2r_4 + q_4r_1r_2r_3, \\
C_2 &= r_1q_2q_3p_4 + r_1q_2p_3q_4 + r_1p_2q_3q_4 - q_1r_2q_3p_4 - \\
&\quad q_1r_2p_3q_4 - p_1r_2q_3q_4 - q_1q_2r_3p_4 - q_1p_2r_3q_4 - \\
&\quad p_1q_2r_3q_4 - r_1r_2r_3p_4 + q_1q_2p_3r_4 + q_1p_2q_3r_4 + \\
&\quad p_1q_2q_3r_4 + r_1r_2p_3r_4 + r_1p_2r_3r_4 - p_1r_2r_3r_4, \\
C_3 &= -r_1q_2p_3p_4 - r_1p_2q_3p_4 - r_1p_2p_3q_4 + q_1r_2p_3p_4 + \\
&\quad p_1r_2q_3p_4 + p_1r_2p_3q_4 + q_1p_2r_3p_4 + p_1q_2r_3q_4 + \\
&\quad p_1p_2r_3q_4 + r_1r_2r_3q_4 - q_1p_2p_3r_4 - p_1q_2p_3r_4 - \\
&\quad p_1p_2q_3r_4 - r_1r_2q_3r_4 - r_1q_2r_3r_4 + q_1r_2r_3r_4, \\
C_4 &= r_1p_2p_3p_4 - p_1r_2p_3p_4 - p_1p_2r_3p_4 - r_1r_2r_3p_4 + \\
&\quad p_1p_2p_3r_4 + r_1r_2p_3r_4 + r_1p_2r_3r_4 - p_1r_2r_3r_4;
\end{aligned} \tag{8}$$

and $\mathbf{S}_{12} = (p_1, q_1, r_1)^T$, $\mathbf{S}_{14} = (p_2, q_2, r_2)^T$, $\mathbf{S}_{23} = (p_3, q_3, r_3)^T$, and $\mathbf{S}_{34} = (p_4, q_4, r_4)^T$ are the coordinates of the vertices of the compatibility linkage.

Given that axes for the central-axis cone are biased toward the $Z > 0$ side of the sphere, the axes on the $Z < 0$ side are easily obtained by negating the original set. Figure 5 shows an example of a central-axis cone generated by `SphinxPC`.

## 3. Type Map Generation

The spherical linkages that solve a specific four-orientation task form a two-dimensional set that is color-coded based on linkage type, and form the *Type Map*. See Figure 6. The resolution of the the Type Map is defined by the number of points, $N$, computed on the central-axis cone.

A given spherical four-bar linkage with vertices **OABC** can be constructed with any combination of the four vectors negated. Thus, there are 16 forms for any given linkage. We bias the four vertices so they are directed toward the $Z > 0$ hemisphere, and denote this form as $(+,+,+,+)$. All other forms of the linkage are obtained by negating combinations of the axes, for example $(-,+,+,+)$ has $\mathbf{O}$ directed toward the $Z < 0$ hemisphere. Type Maps for all 16 forms of the linkage are generated by `SphinxPC`.

The steps required for this phase of the software are: *i)* Construct linkage $L(i,j)$ and *ii)* Evaluate linkage characteristics—specifically linkage type, input drivability, and order.

### 3.1 Construct the Linkage $L(i,j)$

Let $\mathbf{O}_i, i = 1,\ldots,N$ be the set of central-axes. For each of these axes, we determine the associated moving axis $\mathbf{A}_i$ using the constraint equations of the dyad. This is actually done in the moving frame, where for a given fixed axis we obtain a set of linear equations that define the moving axis. The resulting coordinate vector of the moving axis is transformed back to the fixed frame to yield the dyads $\mathbf{O}_i\mathbf{A}_i$. Two dyads $\mathbf{O}_i\mathbf{A}_i$ and $\mathbf{O}_j\mathbf{A}_j$ define the linkage $L(i,j)$. The other 16 forms of the linkage are generated by negating combinations of the fixed and moving axes.

The "$X$" coordinate of the Type Map is the driving crank and the "$Y$" coordinate is the driven crank. Reflection through the diagonal of the figure interchanges the driving and driven cranks. The angular dimensions of the four sides of the spherical linkage are given by:

$$\begin{aligned} \alpha &= \arccos(\mathbf{O}_i \cdot \mathbf{A}_i), \beta = \arccos(\mathbf{O}_j \cdot \mathbf{A}_j), \\ \gamma &= \arccos(\mathbf{O}_i \cdot \mathbf{O}_j), \eta = \arccos(\mathbf{A}_i \cdot \mathbf{A}_j). \end{aligned} \tag{9}$$

For each linkage, we determine the input angles $\theta_k$ and coupler angle $\phi_k$ when the linkage is assembled in each of the four design orientations, $k = 1,2,3,4$. These are easily computed from the coordinates of the axes by the formulas:

$$\begin{aligned}\theta_k &= \arctan \frac{(\mathbf{O}_i \times \mathbf{O}_j) \cdot \mathbf{A}_{ik}}{(\mathbf{O}_i \times \mathbf{O}_j) \cdot (\mathbf{O} \times \mathbf{A}_{ik})}, \\ \phi_k &= \arctan \frac{(\mathbf{O}_i \times \mathbf{A}_{ik}) \cdot \mathbf{A}_{jk}}{(\mathbf{O}_i \times \mathbf{A}_{ik}) \cdot (\mathbf{A}_{ik} \times \mathbf{A}_{jk})}, k = 1, \ldots, 4, \end{aligned} \tag{10}$$

where $\mathbf{A}_{ik}$ is the $i^{th}$ moving axis located in the $k^{th}$ orientation.

### 3.2 Type Determination

The classification of the overall movement of a spherical $4R$ linkage can be described in the terms "crank" and "rocker," in a manner similar to planar linkages. In this context, a crank is a link coupled to the base that completely rotates relative to the base, and a rocker is a similar link that oscillates between limiting positions. Grashoff's criterion identifies the combination of four link lengths that ensure that at least one link can fully rotate. These linkages are said to be *Grashoff* and the remaining are *non-Grashoff*. It is the shortest link in a Grashoff linkage that can fully rotate; therefore, Grashoff linkages are further distinguished by which of the four links is the shortest: *i)* Crank-rocker (input); *ii)* Double-rocker (coupler); *iii)* Rocker-crank (output); and *iv)* Drag-link (ground). The non-Grashoff linkages are grouped together and called *triple rockers*; however, it is possible to further categorize these linkages (Murray 1996).

The presence of 16 variations of the same spherical linkage make the classification procedure a little more difficult. The usual approach is to change the dimensions of the linkage among these variations in order to obtain a "model linkage" for which an spherical version of Grashoff's criterion applies (Chiang 1988). Murray and McCarthy (1995) introduced an alternate approach which uses the actual dimensions of a given spherical linkage.

Consider a spherical linkage with vertices **OABC**. Let $\theta$ be the input angle of the driving link **OA** and $\psi$ the output angle of the driven link **CB**. These angles are related by the condition that $\mathbf{B} \cdot \mathbf{A} = \cos\eta$ in all configurations of the linkage, which yields the constraint equation:

$$A(\theta)\cos\psi + B(\theta)\sin\psi = C(\theta), \tag{11}$$

where

$$\begin{aligned} A(\theta) &= \sin\beta(\sin\alpha\cos\gamma\cos\theta - \sin\gamma\cos\alpha), \\ B(\theta) &= \sin\alpha\sin\beta\sin\theta, \\ C(\theta) &= \cos\eta - \cos\beta(\sin\alpha\sin\gamma\cos\theta + \cos\alpha\cos\gamma). \end{aligned} \tag{12}$$

The solution is:

$$\psi(\theta) = \arctan(\frac{B}{A}) \pm \arccos(\frac{C}{\sqrt{A^2 + B^2}}) \tag{13}$$

Notice that there are two solutions for each value of $\theta$, one obtained for plus and one for minus in this equation. We call these the two *modes* of the solution.

**3.2.1 Crank Rotation Limits.** Notice that in order for a solution to exist the argument to arccos must be in the range $(-1, 1)$. This is equivalent to the condition:

$$A^2(\theta) + B^2(\theta) - C^2(\theta) \geq 0. \tag{14}$$

Set Eq. (14) equal to zero to obtain a quadratic polynomial in $\cos\theta$ with roots:

$$\begin{aligned} C_1 &= \frac{\cos(\eta - \beta) - \cos\alpha\cos\gamma}{\sin\alpha\sin\gamma}, \\ C_2 &= \frac{\cos(\eta + \beta) - \cos\alpha\cos\gamma}{\sin\alpha\sin\gamma}. \end{aligned} \tag{15}$$

These equations are simply the spherical cosine laws for the triangle formed when the coupler and output link are aligned. The root $C_1$ defines the smallest positive angle the input crank can reach, $\theta_{\min}$; the root $C_2$ determines the largest positive angle $\theta_{\max}$. Thus, we have:

$$\theta_{\min} = \arccos C_1, \quad \text{and} \quad \theta_{\max} = \arccos C_2. \tag{16}$$

However, it is possible that $|C_1| \geq 1$, in which case $\theta_{\min} = 0$ and the crank can pass through zero. Similarly, if $|C_2| \geq 1$ then $\theta_{\max} = \pi$ and the crank can pass through $\pi$.

A detailed study of Eq. (15) leads to the introduction of four parameters (Murray and McCarthy 1995):

$$\begin{aligned} T_1 &= \gamma - \alpha + \eta - \beta, T_2 = \gamma - \alpha - \eta + \beta, \\ T_3 &= \eta + \beta - \gamma - \alpha, \quad \text{and} \quad T_4 = 2\pi - (\eta + \beta + \gamma + \alpha). \end{aligned} \tag{17}$$

These parameters characterize the movement of the driving link as follows:

1. $T_1T_2 > 0$ and $T_3T_4 > 0$, the driving link fully rotates.
2. $T_1T_2 > 0$ and $T_3T_4 < 0$, the driving link rocks through $\theta = 0$.
3. $T_1T_2 < 0$ and $T_3T_4 > 0$, the driving link rocks through $\theta = \pi$.
4. $T_1T_2 < 0$ and $T_3T_4 < 0$, the driving link rocks over two ranges, neither of which includes 0 or $\pi$.

An analysis of the linkage in terms of the driven link angle $\psi$ shows that the same parameters characterize the movement of the driven link:

1. $T_2T_4 < 0$ and $T_1T_3 < 0$, the driven link fully rotates.
2. $T_2T_4 < 0$ and $T_1T_3 > 0$, the driven link rocks through $\psi = 0$.
3. $T_2T_4 > 0$ and $T_1T_3 < 0$, the driven link rocks through $\psi = \pi$.
4. $T_2T_4 > 0$ and $T_1T_3 > 0$, the driven link rocks over two ranges, neither of which includes 0 or $\pi$.

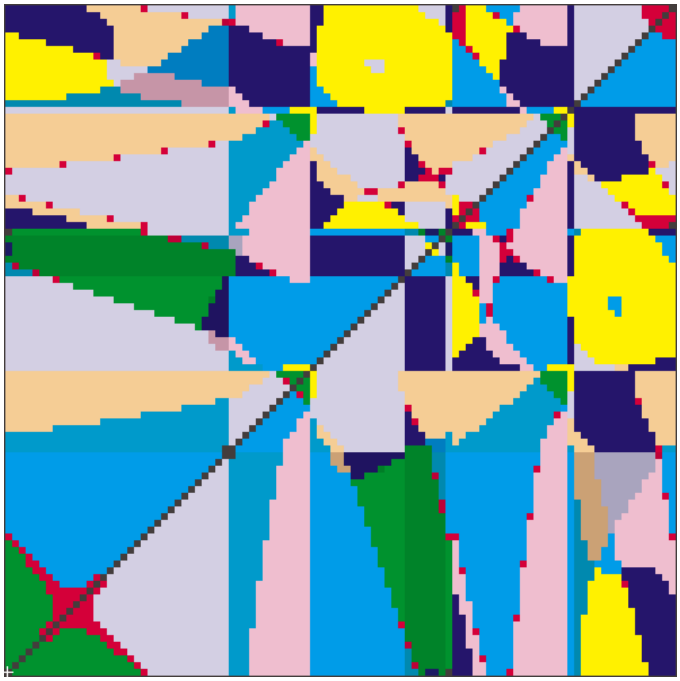

**Fig. 6.** The set of linkages assembled from pairs of axes on the central-axis cone, color-coded for type, forms the Type Map.

**3.2.2 The Parameters $T_i$.** Let the function $\sigma(T_i)$ take on values $+1$, $-1$, or 0 depending on whether $T_i$ is positive, negative or zero. This allows us to identify a signature $(\sigma(T_1), \sigma(T_2), \sigma(T_3), \sigma(T_4)$ for each spherical linkage, which we call its *type*.

It is easy to see that there are 81 spherical-linkage types, which can be separated into three general categories depending on the value of $\sigma(T_4)$. If $\sigma(T_4) = +1$, then the sum of the four angular link lengths is less than $2\pi$. This means the linkage lies on one side of the sphere. There are 27 spherical-linkage types in this category which are equivalent to the well-known planar-linkage types. If $\sigma(T_4) = -1$, then the angular lengths of the four links add up to greater than $2\pi$, and the linkage must wrap around the sphere. There are 27 linkage types in this category, which can be related to analogous planar-linkage types. Finally, there are 27 types for which $\sigma(T_4) = 0$. These linkages have a configuration in which the links can align to form a great circle on the sphere.

If any of the parameters $T_i$, for $i = 1, 2, 3, 4$, is zero, the linkage can collapse so that its axes become co-planar. These linkages are said to *fold*. Thus, there are 65 types of folding spherical linkages. The number of the parameters $T_i$ that equal zero is the number of folding configurations. For

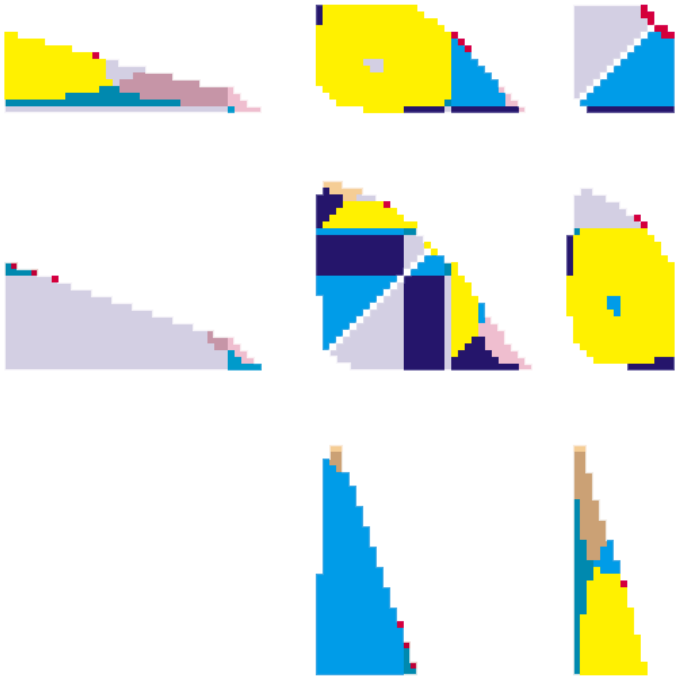

**Fig. 7.** The spherical linkage Type Map with the "input-drivable" and "order" filters applied.

example, the spherical rhombus with four sides of dimension $\frac{\pi}{2}$, the only linkage of type $(0, 0, 0, 0)$, has four folding configurations.

The 16 non-folding linkage types divide such that eight lie on one side of the sphere ($\sigma(T_4) = +1$) and eight wrap around the sphere ($\sigma(T_4) = -1$). The eight types in each category pair up to become the well-known four Grashoff linkages and the four triple rockers obtained using the classification scheme of Chiang (1988).

### 3.3 Evaluate Linkage Characteristics

For each linkage $L(i, j)$, we evaluate the parameters $T_i$ and assign a color to represent the type. In addition, the designer can apply *filters* to eliminate linkages that have order and branching defects.

The color scheme for the Type Map uses shades of blue to represent non-Grashoff linkages, red to identify folding linkages, and other colors (yellow, orange, pink, and green) to represent the Grashoff linkages. We add black to obtain a darkened version of the same color scheme to identify linkages that wrap around the sphere.

The evaluation of branching defects consists of a series of checks. The first step is to determine that all of the goal positions are on the same solu-

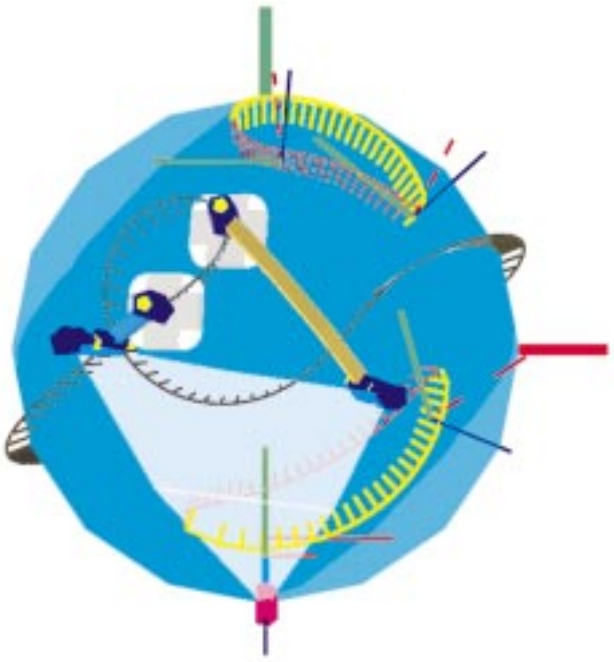

**Fig. 8.** The animation of a spherical linkage guiding its goal frame along a coupler curve is a useful evaluation tool.

tion of the linkage, non-Grashoff linkages that meet this criterion are called *input-drivable*. This means the driving crank will move the coupler smoothly through the four positions without jamming. For Grashoff linkages, the same linkage solution can be divided over two ranges of motion of the crank, so we must also check that the goal positions are reached from one range. Satisfying this check defines input-drivable Grashoff linkages. All linkages that are not input-drivable are flagged. The designer can eliminate them from consideration by selecting the input-drivable filter on the Type Map.

The order check determines if the linkage moves through the goal orientations in the specified order. Linkages that are not ordered are flagged and can be eliminated from the Type Map by applying the order filter. Figure 7 shows the type map with the input-drivable and order filters applied.

## 4. Design Selection

The designer interacts directly with the Type Map to select a linkage $L(i, j)$ and examine its characteristics. The detailed properties of this linkage are displayed in the Design Information dialog box. The primary tools for evaluation of a linkage are the display of its coupler curve, and the animation of

its movement as it guides the moving frame along the coupler curve through the desired orientations. The operations of this phase of the software are: *i)* Analyze the linkage $L(i, j)$; and *ii)* Generate the display information.

Given the selection $L(i, j)$ on the Type Map, the software computes and displays the coupler curve, coded for the two solution modes. The arrow keys allow movement in the vertical and horizontal direction of the Type Map so a sequence of linkages and their evolving coupler curves can be viewed. This provides useful insight into characteristics of the task—see Figure 8, which shows a spherical linkage with its coupler curve.

An animation dialog box provides VCR style buttons to animate the linkage in forward and reverse directions with pause and fast forward. This provides a view of the linkage guiding the moving body through the desired positions. Various bias schemes for the joint axes provide different configurations for the movement of the supporting links.

There are also buttons to toggle between the two modes of solution as well as between the two assemblies available for Grashoff linkages. It is important to realize that while the separate circuits of a Grashoff linkage may correspond to separate modes of solution, it is also possible for the two solution modes to exist on each circuit (Fig. 8).

In the process of specifying a task and examining the resulting linkage designs, we have found that the designer develops a perception in the characteristics of the task that impact desirable features of these designs. This insight often directs a modification of the task that results in a larger set of acceptable linkages. While it seems to be easily done by the designer, we have yet to formulate a mathematical version of this strategy. Enhancing this capability for the designer may be fundamental to the success of spatial linkage design tools.

## 5. Conclusion

This chapter described the implementation of spherical four-orientation synthesis in the software `SphinxPC`. The software encodes a new formulation of classical Burmester theory based on the equation of a spherical triangle which yields a convenient parameterized equation for the central-axis cone. The linkage Type Map is used to provide a convenient means to display and evaluate the characteristics of the two-dimensional set of solutions to the four-orientation synthesis problem. The result is a design tool which, in the hands of students at several universities, has yielded spherical linkages that achieve a wide variety of spatial reorientation tasks.

## 6. Acknowledgment

The authors gratefully acknowledge the support of the National Science Foundation grant DMII9321936 and the contributions of Mohan Bodduluri, Pierre Larochelle and Andrew Murray to the evolution of the Sphinx linkage design software over the past decade.

## References

Bottema, O., and Roth, B. (1979): *Theoretical Kinematics*. North-Holland Publishing Company, New York.

Burmester, L. (1886): *Lehrbuch der Kinematik*. Verlag Von Arthur Felix, Leipzig, Germany.

Chiang, C. H. (1988): *Kinematics of Spherical Mechanisms*. Cambridge Univ. Press.

Erdman, A., and Gustafson, J. (1977): LINCAGES: Linkage INteractive Computer Analysis and Graphically Enhanced Synthesis Packages, Technical Report 77-DET-5, American Society of Mechanical Engineers.

Erdman, A. G. (1993): *Modern Kinematics: Developments in the Last Forty Years*. John Wiley and Sons, Inc., New York.

Hall, A. S., Jr. (1961): *Kinematics and Linkage Design*. Prentice-Hall, Inc., Englewood Cliffs, New Jersey.

Kaufman, R. (1978): Mechanism Design by Computer, *Machine Design*. pp. 94-100.

McCarthy, J. M. (1993): The Opposite Pole Quadrilateral as a Compatibility Linkage for Parameterizing the Center Point Curve. *ASME Journal of Mechanical Design*. 115(2):332-336.

McCarthy, J. M., The Synthesis of Planar RR and Spatial CC Chains and the equation of a Triangle. *Transactions of the ASME - Special 50th Anniversary Design Issue*. 117:101-106.

Murray, A. P., and McCarthy, J. M. (1994): Five Position Synthesis of Spatial CC Dyads, *Proc. ASME Mechanisms Conference* Minneapolis, MN, Sept.

Murray, A. P., and McCarthy, J. M. (1995): A Linkage Type Map for Spherical 4 Position Synthesis, *Proceedings of the 1995 ASME Design Technical Conferences*. Boston, MA, Sept.

Murray, A. P. (1996): *Global Properties of Constraint Manifolds in the Kinematic Synthesis of Closed Chains*. PhD Thesis, University of California, Irvine.

Roth, B. (1967): On the Screw Axes and Other Special Lines Associated with Spatial Displacements of a Rigid Body. *ASME Journal of Engineering for Industry*. February.

Sandor, G. N., and Erdman, A. G. (1984): *Advanced Mechanism Design: Analysis and Synthesis*. Vol. 2, Prentice-Hall, Inc., Englewood Cliffs, New Jersey.

Suh, C. H., and Radcliffe, C. W. (1978): *Kinematics and Mechanism Design*. John Wiley and Sons, New York.

Waldron, K. J., and Song, S. M. (1981): Theoretical and Numerical Improvements to an Interactive Linkage Design Program, RECSYN, *Proceedings of the Seventh Applied Mechanisms Conference*, Kansas City, Missouri, December.